Solvation Dynamics in the Water Pool of an Aerosol-OT Microemulsion. Effect of Sodium Salicylate and Sodium Cholate

Partha Dutta, Pratik Sen, Saptarshi Mukherjee, Arnab Halder, and Kankan Bhattacharyya*

Physical Chemistry Department, Indian Association for the Cultivation of Science, Jadavpur, Kolkata 700 032, India

Received: January 22, 2003; In Final Form: May 28, 2003

The effect of sodium salicylate (Na-sal) and sodium cholate (Na-cholate) on the solvation dynamics in the water pool of aerosol-OT (AOT, sodium dioctylsulfosuccinate) microemulsion in *n*-heptane is reported. In the absence of any additive, the solvation dynamics of 4-(dicyanomethylene)-2-methyl-6-(*p*-dimethylaminostyryl)-4*H*-pyran (DCM) in AOT microemulsions is found to be biexponential with an average solvation time ($\langle\tau_s\rangle$) of 710 ps. In the water pool, $\langle\tau_s\rangle$ decreases to 330 ps on addition of 1 mM Na-sal and increases to 3050 ps in the presence of 100 mM Na-cholate. The spectral width (Γ) of the time-resolved emission spectra of DCM in the water pool is found to be time dependent. This is ascribed to diffusion of the probe (DCM). The Na-sal-induced acceleration of the solvation dynamics is ascribed to the increase in the size of the water pool. In bulk water, in the presence of 100 mM Na-cholate (a bile salt), $\langle\tau_s\rangle$ is ∼830 ps. This is 4 times shorter than $\langle\tau_s\rangle$ in the presence of Na-cholate in the water pool. This is ascribed to extreme crowding in the water pool because of the presence of Na-cholate aggregates. In bulk water, the emission spectral width displays a very small time dependence in the presence of Na-cholate aggregates. This suggests that in this case self-diffusion is unimportant and the slow solvation arises entirely from the dynamic exchange.

1. Introduction

Interactions of biological macromolecules with various species in a confined aqueous volume ("water pool") play fundamental roles in many biological processes. The water molecules confined in the water pool differ in a number of ways from bulk water. Recently, it has been reported that the solvation dynamics of the confined water molecules in a protein,[1] DNA,[2] microemulsions,[3−5] lipid vesicles,[6] polymers,[7] and a sol−gel glass[8,9] displays a component which is markedly slower compared to that of bulk water.[8,13] Similar slow components of relaxation dynamics in confined systems have been detected using NMR,[10] and have been predicted in analytical theory,[11] and recent computer simulations.[12]

A microemulsion containing a surfactant-coated water droplet (water pool) is an elegant model of confined water molecules.[14−24] Microemulsions involving the anionic surfactant AOT (sodium dioctylsulfosuccinate, aerosol-OT) has been studied extensively using many techniques.[14−24] Amararene et al. reported that, even in a large water pool ($w_0 = 27$), the compressibility is 2 times larger than that in bulk water.[20] The libration frequency at 670 cm^{-1} in bulk water exhibits a 25% shift in the water pool of the AOT microemulsion.[21] The terahertz (THz) absorption spectrum of the confined water molecules in the water pool in the region 0.1−1.3 THz is very different from that of bulk water.[24] The integrated area of absorption for the confined water molecules is significantly smaller compared to that of bulk water even at large w_0.[24] The absorption in the terahertz frequencies shifts from about 25 cm^{-1} in a water pool of radius 1.5 nm to less than 10 cm^{-1} for a water pool of radius 2.9 nm.[24a]

With an increase in the ratio (w_0) of the number of molecules of water and AOT, the radius of the water pool (r_w) increases according to the relation r_w (nm) ≈ $0.15w_0$.[15−19] The hydrodynamic radius (r_h) of a microemulsion is equal to $r_w + d$, where d denotes the thickness of the hydrated surfactant layer. d is roughly equal to the sum of the length of an AOT molecule (1.2 nm) and one water layer (0.2 nm),[33d] and thus, $d \approx 1.5$ nm. Many authors[14−19] used the relation r_h (nm) = $r_w + 1.5 \approx 0.15w_0 + 1.5$. Different additives markedly affect r_h and r_w. Nazario et al.[19] observed that addition of alkanols causes a reduction while addition of polyoxyethylene alkyl ethers causes an increase in r_h and r_w. Moulik et al.[18] studied the effect of sodium salicylate (Na-sal) and sodium cholate (Na-cholate) (Chart 1) on the size of the water pool of an AOT microemulsion. At 300 K, at $w_0 = 39.5$, r_h is 6.8 nm and r_w is 5.3 nm.[18] On addition of 1 mM Na-sal to the AOT microemulsion r_h increases about 4 times to 25.8 nm and r_w to 24.3 nm.[18] Addition of 100 mM Na-cholate to AOT at $w_0 = 39.5$ however causes a relatively smaller increase of r_h to 12 nm and of r_w to 10.5 nm.[18] We have previously reported a nonmonotonic variation of the size of an AOT microemulsion on addition of a polymer, poly(vinylpyrrolidone) (PVP).[4e] Many different mechanisms such as shape fluctuations,[14,18,19,22] clustering,[18] and polydispersity[15−19,22] have been proposed to explain the effect of the different additives on the microemulsion. In this work, we investigate this phenomenon using solvation dynamics.

In bulk water, the solvation dynamics occurs with a major component on a less than 0.1 ps time scale and a small component of ∼1 ps.[25] In the confined water pool of the AOT microemulsions, the solvation dynamics slows dramatically.[3,4] Levinger et al. showed that in lecithin and an AOT microemulsion there is a long component on a 100 ps time scale.[3] This component becomes faster as w_0 increases.[3] Several other groups have reported a slow component of the solvation dynamics on a 100−1000 ps time scale in microemulsions.[4] It should be noted that a similar retardation of the solvation dynamics by 2−3

* To whom correspondence should be addressed. E-mail: pckb@mahendra.iacs.res.in. Fax: (91)-33-2473-2805.

10.1021/jp030083g CCC: $25.00
Published on Web 09/06/2003

CHART 1: Structure of (a) DCM and (b) Na-cholate

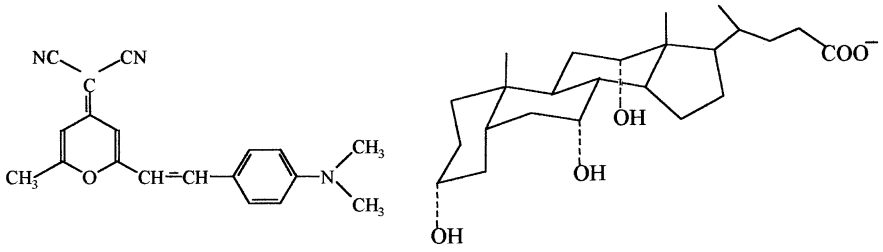

orders of magnitude compared to that of bulk liquid is also observed for several nonaqueous solvents confined inside an AOT microemulsion.[5]

We report here the effect of two additives, Na-sal and Na-cholate, on the solvation dynamics of the laser dye 4-(dicyanomethylene)-2-methyl-6-(*p*-dimethylaminostyryl)-4*H*-pyran[26,27] (DCM, Chart 1) inside the water pool of an AOT microemulsion. The additives are chosen because they modify the size of AOT microemulsions.[18] Another objective is to study the aggregation of Na-cholate within the water pool. Like other bile salts Na-cholate exhibits two critical micellar concentrations (CMCs).[28,29] At around 15 mM, Na-cholate forms primary micellar aggregates (micelles), and above 50 mM, secondary aggregates are formed.[29] In this work, we have compared the solvation dynamics of DCM in 100 mM Na-cholate in bulk water and in the water pool.

In an AOT microemulsion, the DCM molecules reside both in bulk *n*-heptane and inside the water pool.[4a] At the wavelength of our laser (405 nm), the DCM molecules both in bulk *n*-heptane and inside the water pool are excited. However, the contribution of DCM molecules in *n*-heptane to the total emission is very small because of a significant blue shift of the emission maximum and a markedly weaker emission intensity compared to those of DCM in the water pool.[4a] Further, DCM does not show a dynamic Stokes shift in *n*-heptane. Thus, the solvation dynamics reported in this work arises exclusively from the DCM molecules in the water pool.

In an attempt to understand how solvent−solute interaction (i.e., solvation) affects rotational motion of the solute (probe), Maroncelli et al. carried out a very detailed analysis of the rotational dynamics and solvation dynamics of a single dye in many liquids.[30a] They detected a nonexponential decay of the fluorescence anisotropy even in many simple liquids. Also they found that there is a clear difference between nonpolar (alkane) and polar solvents. They observed that the existing theoretical models are inadequate even for simple liquids. An organized assembly (e.g., a reverse micelle) involves an interface between nonpolar and polar liquids and is more complex than a simple liquid. In such an assembly, the situation is further complicated by the superposition of the motion of the surfactants and overall rotation of the aggregate on the rotational motion of the fluorescent probe. Thus, in the present work we focus our attention only on solvation dynamics, which reports exclusively the motion of the confined solvent (water) molecules.

2. Experimental Section

DCM (laser grade, Exciton), AOT (Aldrich), Na-sal (Merck), and Na-cholate (Sigma) were used as received. To a solution of DCM in *n*-heptane was added a calculated amount of solid AOT (1.5 g of AOT to 8 mL of *n*-heptane).[18] Then pure water or 1 mM Na-sal solution was added using a microliter syringe. Solid Na-cholate was added to the AOT microemulsion. The steady-state absorption and emission spectra were recorded on a JASCO 7850 spectrophotometer and a Perkin-Elmer 44B spectrofluorimeter, respectively. For lifetime measurements, the samples were excited at 405 nm using a picosecond diode (IBH Nanoled-07). The emission was collected at a magic angle polarization using a Hamamatsu MCP photomultiplier (2809U). The time-correlated single-photon counting (TCSPC) setup consists of an Ortec 935 QUAD CFD and a Tennelec TC 863 TAC. The data are collected with a PCA3 card (Oxford) as a multichannel analyzer. The typical full width at half-maximum (fwhm) of the system response is about 80 ps.

3. Results

3.1. Steady-State Spectra. Figure 1 shows the difference between the absorption spectra of DCM in an AOT microemulsion in the presence of 100 mM Na-cholate and that in *n*-heptane alone. As reported earlier for AOT alone,[4a] the difference spectrum displays negative absorption at 430 nm and a distinct positive peak at 495 nm. The negative absorption at 430 nm clearly indicates that, on addition of AOT and water, the population of DCM in bulk *n*-heptane decreases and the population of DCM inside the water pool increases. The positive peak at 495 nm is assigned to the DCM molecules in a highly polar region inside the water pool. Thus, the difference spectrum reveals migration of DCM from bulk *n*-heptane to the interior of the water pool. Similar difference spectra and migration are also observed in the presence of Na-sal in an AOT microemulsion.

In the absence of water, i.e., in the AOT reverse micelle with $w_0 = 0$, DCM exhibits an emission maximum at 550 nm.[4a] On addition of water to the AOT reverse micelle, the emission maximum of DCM shows a marked red shift to 615 nm at $w_0 = 39.5$. The latter is very similar to the emission maximum of

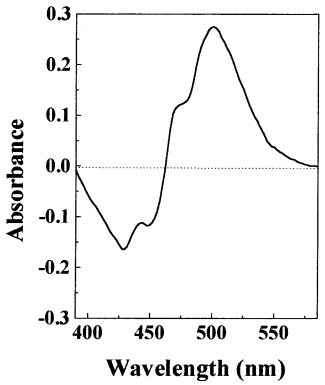

Figure 1. Difference between the absorption spectrum of DCM in an *n*-heptane solution containing 1.5 g of AOT in 8 mL of *n*-heptane and 100 mM Na-cholate at $w_0 = 39.5$ and that of DCM in *n*-heptane.

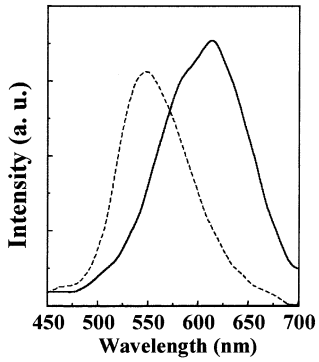

Figure 2. Steady-state emission spectra of DCM in 1.5 g of AOT in 8 mL of *n*-heptane at $w_0 = 0$ (---) and in the presence of 100 mM Na-cholate in 1.5 g of AOT in 8 mL of *n*-heptane at $w_0 = 39.5$ (—).

DCM in methanol.[26,27] The emission maximum and intensity of DCM in the microemulsion ($w_0 = 39.5$) do not change on addition of 1 mM Na-sal or 100 mM Na-cholate (Figure 2).

DCM is insoluble in water and remains so in 1 mM Na-sal. However, in the presence of 100 mM Na-cholate, DCM dissolves in water and exhibits an emission maximum at 615 nm. The 615 nm emission band is ascribed to DCM molecules inside the Na-cholate micelles in bulk water.

3.2. Time-Resolved Studies. *3.2.1. Solvation Dynamics of DCM in an AOT Microemulsion at $w_0 = 39.5$.* The fluorescence decays of DCM in the water pool of an AOT microemulsion at $w_0 = 39.5$ are found to be markedly dependent on the emission wavelength. For example, at the blue end, 530 nm, the fluorescence decay is biexponential with two decay components of 140 ps (93%) and 840 ps (7%), while at the red end, 700 nm, the decay of time constant 1.48 ns is preceded by a distinct rise with a time constant of 230 ps. Following the procedure given by Fleming and Maroncelli,[30b] the TRES (time-resolved emission spectra) were constructed using the parameters of best fit to the fluorescence decays and the steady-state emission spectrum. The solvation dynamics is described by the decay of the solvent correlation function $C(t)$, defined as

$$C(t) = \frac{\nu(t) - \nu(\infty)}{\nu(0) - \nu(\infty)}$$

where $\nu(0)$, $\nu(t)$, and $\nu(\infty)$ are the peak frequencies at time 0, t, and ∞, respectively. $\nu(\infty)$ is obtained by fitting $\nu(t)$ to time t as $\nu(t) = \nu(\infty) + [\nu(0) - \nu(\infty)]\{\sum a_i \exp(-t/\tau_i)\}$. According to this equation, decay of $C(t)$ is biexponential; i.e., $C(t) = \sum a_i \exp(-t/\tau_i)$. The plot of $\nu(t)$ against t is shown in Figure 3a. Figure 3b shows the decay of $C(t)$. The decay parameters of $C(t)$ (i.e., a_i and τ_i) are summarized in Table 1. At $w_0 = 39.5$, in an AOT microemulsion, the decay of $C(t)$ is biexponential with one component of 240 ps (83%) and a slow component of 3000 ps (17%). The average solvation time ($\langle\tau_s\rangle = \sum a_i\tau_i$) is found to be 710 ps. The total Stokes shift for DCM in an AOT microemulsion at $w_0 = 39.5$ is 1975 cm^{-1}.

As reported earlier,[4a] in an AOT microemulsion the emission spectrum of DCM exhibits a time-dependent spectral width (Γ). Γ is defined as full width at half maximum (FWHM). We will discuss this issue in detail in section 3.2.5.

3.2.2. Solvation Dynamics of DCM in an AOT Microemulsion at $w_0 = 39.5$ in the Presence of 1 mM Na-sal. In the presence of 1 mM Na-sal in an AOT microemulsion at $w_0 = 39.5$, the fluorescence decay of DCM at 530 nm (blue end) is fitted to a biexponential with two components of 125 ps (93%) and 780 ps (7%). At 700 nm (red end), DCM exhibits a decay component of 1.47 ns and a distinct rise of 290 ps. The decay of $C(t)$ for

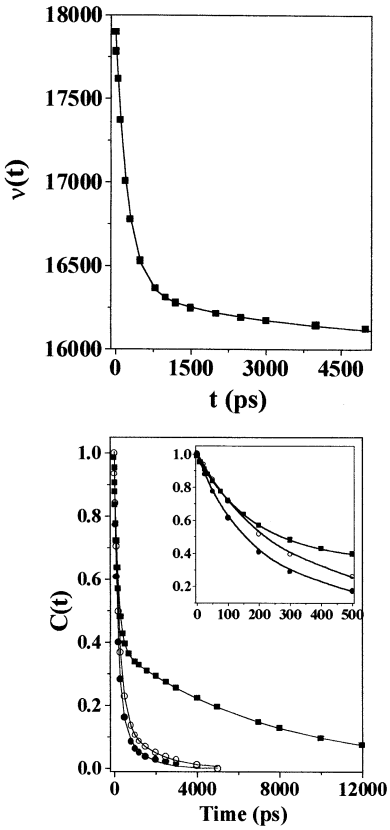

Figure 3. (a, top) $\nu(t)$ against t for DCM in 1.5 g of AOT in 8 mL of *n*-heptane at $w_0 = 39.5$ (■). The points denote the actual values of $\nu(t)$, and the solid line denotes the best fit to a biexponential decay. (b, bottom) Decay of the response function $C(t)$ of DCM in 1.5 g of AOT in 8 mL of *n*-heptane at $w_0 = 39.5$ (○), in 1 mM Na-sal in the same water pool of $w_0 = 39.5$ (●), and in 100 mM Na-cholate in the same water pool of $w_0 = 39.5$ (■). The points denote the actual values of $C(t)$, and the solid line denotes the best fit to a biexponential decay. The initial parts of the decays of $C(t)$ are shown in the inset.

TABLE 1: Decay Parameters of $C(t)$ of DCM in an AOT Microemulsion (1.5 g of AOT in 8 mL of *n*-Heptane) at $w_0 = 39.5$ and in Bulk Water

system	$\Delta\nu^a$ (cm^{-1})	a_1	$\tau_1{}^a$ (ps)	a_2	$\tau_2{}^a$ (ps)	$\langle\tau_s\rangle^{a,b}$ (ps)
AOT	1975	0.83	240	0.17	3000	710
AOT + 1 mM Na-sal	1880	0.82	170	0.18	1050	330
AOT + 100 mM Na-cholate	2750	0.60	180	0.40	7360	3050
100 mM Na-cholate in bulk water	580	0.88	380	0.12	4150	830

[a] ±10%. [b] $\langle\tau_s\rangle = a_1\tau_1 + a_2\tau_2$.

DCM in the presence of 1 mM Na-sal in an AOT microemulsion at $w_0 = 39.5$ is found to be biexponential with one component of 170 ps (82%) and another of 1050 ps (18%), with an average solvation time of 330 ps. This is about 2 times faster than that in DCM in an AOT microemulsion at $w_0 = 39.5$ in the absence of Na-sal (Figure 3b, Table 1). The total Stokes shift is observed to be 1880 cm^{-1}.

In the presence of 1 mM Na-sal in an AOT microemulsion, the spectral width of the emission spectrum of DCM is found to be time dependent. We will discuss this in section 3.2.5.

3.2.3. Solvation Dynamics of DCM in the Presence of 100 mM Na-cholate in an AOT Microemulsion at $w_0 = 39.5$. In the presence of 100 mM Na-cholate in an AOT microemulsion at $w_0 = 39.5$, at the blue end, 530 nm, the fluorescence decay of DCM is biexponential with two decay components of 140 ps (92%) and 850 ps (8%) (Figure 4). At the red end (700 nm) the decay of time constant 1.53 ns is preceded by a distinct rise

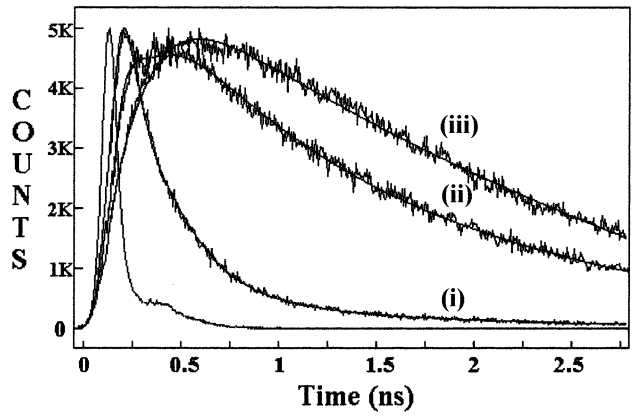

Figure 4. Fluorescence decays of DCM in the presence of 100 mM Na-cholate in 1.5 g of AOT in 8 mL of *n*-heptane at $w_0 = 39.5$ at (i) 530 nm, (ii) 615 nm, and (iii) 700 nm.

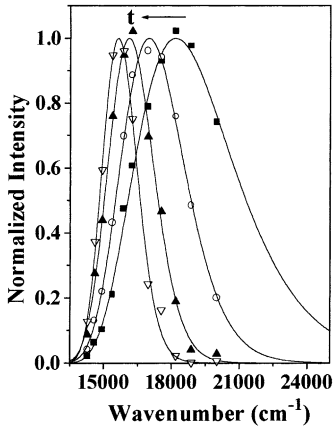

Figure 5. Time-resolved emission spectra of DCM in the presence of 100 mM Na-cholate in 1.5 g of AOT in 8 mL of *n*-heptane at $w_0 = 39.5$ at 0 ps (■), 200 ps (○), 3000 ps (▲), and 12000 ps (▽).

with a time constant of 315 ps. The emission spectra show a time-dependent Stokes shift (Figure 5). The decay of $C(t)$ of DCM in the presence of 100 mM Na-cholate in an AOT microemulsion at $w_0 = 39.5$ is found to be biexponential with one component of 180 ps (60%) and a very slow component of 7360 ps (40%) (Figure 3b, Table 1). The average solvation time is found to be 3050 ps. This is about 4 times slower than that in DCM in an AOT microemulsion at $w_0 = 39.5$ in the absence of Na-cholate. The total Stokes shift is found to be 2750 cm^{-1}.

From Figure 5 it is apparent that the width of the emission spectrum for DCM in AOT microemulsions containing Na-cholate decreases with an increase in time from 5100 cm^{-1} at $t = 0$ ns to 1810 cm^{-1} at $t = 12$ ns. This will be discussed elaborately in section 3.2.5.

3.2.4. Solvation Dynamics of DCM in 100 mM Na-cholate in Bulk Water. Since DCM is insoluble in bulk water and in the presence of 1 mM Na-sal, the effect of Na-sal on the solvation dynamics of DCM in bulk water could not be studied.

To compare the effect of Na-cholate in the water pool and in bulk water, the solvation dynamics of DCM was also studied in 100 mM Na-cholate in bulk water. The fluorescence decays of DCM in a solution containing 100 mM Na-cholate in bulk water are shown in Figure 6. In this case the decay at 545 nm (blue end) is fitted to a biexponential with two components of 360 ps (69%) and 2.03 ns (31%). However, at 700 nm (red end), the sample exhibits a decay component of 2.41 ns and a distinct rise of 490 ps. The emission spectra clearly show a time-dependent Stokes shift (Figure 7). The decay of $C(t)$ for DCM

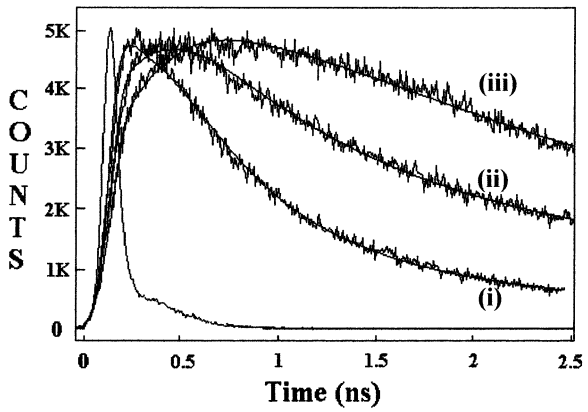

Figure 6. Fluorescence decays of DCM in an aqueous solution containing 100 mM Na-cholate at (i) 545 nm, (ii) 600 nm, and (iii) 700 nm.

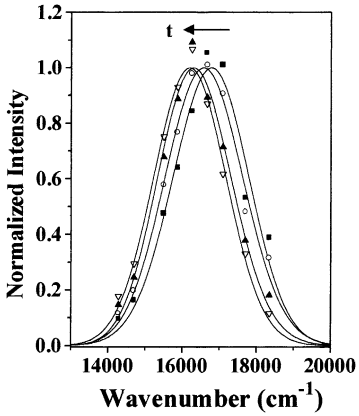

Figure 7. Time-resolved emission spectra of DCM in an aqueous solution containing 100 mM Na-cholate at 0 ps (■), 200 ps (○), 800 ps (▲), and 4000 ps (▽).

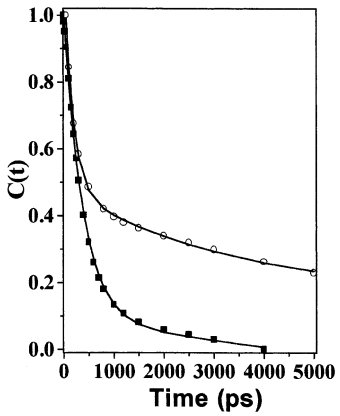

Figure 8. Decay of the response function $C(t)$ of DCM in an aqueous solution containing 100 mM Na-cholate (■) and in the water pool of $w_0 = 39.5$ (○). The points denote the actual values of $C(t)$, and the solid line denotes the best fit to a biexponential decay.

in 100 mM Na-cholate solution in bulk water is found to be biexponential with one component of 380 ps (88%) and another of 4150 ps (12%), with an average solvation time of 830 ps (Figure 8, Table 1). The total Stokes shift is found to be 580 cm^{-1}.

The solvation time of DCM in 100 mM Na-cholate in bulk water is about 4 times faster than that in the water pool of the microemulsion at $w_0 = 39.5$ in the presence of 100 mM Na-cholate. Thus, the microenvironment inside the water pool of microemulsions in the presence of 100 mM Na-cholate is much more restricted than that in the absence of Na-cholate

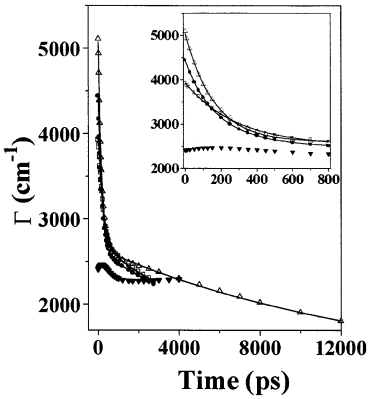

Figure 9. FWHM (Γ) of the emission spectrum against time for DCM in 1.5 g of AOT in 8 mL of *n*-heptane at $w_0 = 39.5$ with no additives (□), with 1 mM Na-sal (●), and with 100 mM Na-cholate (△) and for DCM in the presence of 100 mM Na-cholate in bulk water (▼). The points denote the actual values of Γ, and the solid line denotes the best fit to a biexponential decay. The initial parts of the decays of Γ are shown in the inset.

TABLE 2: Decay Parameters of FWHM (Γ) of the TRES of DCM in Different Systems

system	a_1	τ_1[a] (ps)	a_2	τ_2[a] (ps)	$\langle\tau_\Gamma\rangle$[a,b] (ps)
AOT	0.69	240	0.31	1800	725
AOT + 1 mM Na-sal	0.76	150	0.24	1100	380
AOT + 100 mM Na-cholate	0.68	155	0.32	9100	3020

[a] ±10%. [b] $\langle\tau_\Gamma\rangle = a_1\tau_1 + a_2\tau_2$.

inside the water pool of microemulsions or that in a 100 mM Na-cholate solution in bulk water.

As is evident from the TRES (Figure 7), in bulk water the emission spectral width of DCM does not exhibit appreciable time dependence in the presence of 100 mM Na-cholate. This is in contrast to the case of AOT microemulsions.

3.2.5. Time-Dependent Spectral Width of DCM in AOT Microemulsions. In a simple liquid, the FWHM (Γ) of the emission spectrum changes by a small amount (10−20%) with time.[30a] Maroncelli discussed that in many liquids the emission spectral width (Γ) shows an initial increase followed by a decay.[30c] The major source of the width of the emission spectra is the fluctuations in the local solvent environment.[30c] In a simple liquid the variation of the local solvent environment is small, and hence, the variation of Γ with time is small.

The time dependence of Γ in the various environments is shown in Figure 9. From Figure 9, it is evident that in the microemulsions Γ exhibits a dramatic decrease with an increase in time by over 50%. However, in the case of aggregates of Na-cholate in bulk water, Γ does not change much with time and the time dependence of Γ is similar to that in simple liquids.

We fitted the decay of Γ in AOT microemulsions to a biexponential decay in the absence of any additives and in the presence of the two additives. The results are summarized in Table 2. It may be noted that very recently Hof et al.[6a] reported a similar time dependence of Γ in lipid vesicles. They, however, did not provide any explanation for this. We will attempt to find the origin of the time-dependent width in the following section.

4. Discussion

This work demonstrates that the solvation dynamics in the water pool of an AOT microemulsion becomes 2 times faster on addition of 1 mM Na-sal and 4-fold slower on addition of 100 mM Na-cholate. The solvation dynamics in the presence of 100 mM Na-cholate in the water pool is 4 times slower than that in 100 mM Na-cholate in bulk water. Another interesting observation is the marked time-dependent decrease of Γ in a microemulsion.

Since both the additives are ionic in nature, we first consider the possibility of solvation dynamics by the added ions. Huppert et al. pointed out that solvation by ions may give rise to a nanosecond component of the solvation dynamics.[31] It may be emphasized that the AOT microemulsion contains a lot of sodium ions. At $w_0 = 39.5$, the aggregation number of AOT is 965,[15,17] and hence, there are 965 sodium ions per water pool. On addition of Na-sal the radius of the water pool increases from 5.3 to 24.3 nm. Thus, on addition of 1 mM Na-sal, the volume of the water pool increases in the ratio $24.3/5.3^3$ or 96 times, and in each water pool there are $965 \times 96 \approx 92000$ sodium ions due to AOT and only 132 ions due to Na-sal. In the case of 100 mM Na-cholate, r_w increases from 5.3 to 10.5 nm, and hence, in each water pool there are 7720 sodium ions due to AOT and 1100 ions due to Na-cholate. In both the cases, the amount of added ions (from Na-sal and Na-cholate) is much smaller than that (of sodium ions) already existing in the water pool. The solvation dynamics[32] and terahertz absorption[24a] of microemulsions involving neutral surfactants with no ions in the water pool are very similar to those in an ionic microemulsion. This also suggests that the ions have little or no influence on terahertz absorption as well as the solvation dynamics in the water pool.

Several authors proposed that the additives may affect volume-conserving shape fluctuations of AOT microemulsions.[14,18,19] According to Boyd et al. absorption in the terahertz region, which corresponds to a few picoseconds, arises from the shape fluctuations.[24a] It is obvious that shape fluctuations (occurring in a few picoseconds) are too fast to account for the 100−1000 ps component of the solvation dynamics detected in this work.

In a large water pool of a microemulsion the dielectric relaxation consists of an ultrafast (≤1 ps time scale) bulk-water-like response[24] and a slow (100−1000 ps) component.[23] In bulk water, the ultrafast components of the solvation dynamics and dielectric relaxation have been attributed to the low-frequency libration and intermolecular vibrations.[25c] Thus, the bulk-water-like far-IR spectrum of the intermicellar water[21] is consistent with the ultrafast component of dielectric relaxation[24] and the solvation dynamics[3] in the water pool. However, the slow (100−1000 ps) component of solvation[4] and dielectric relaxation[23] observed in a water pool cannot be attributed to the bulk-water-like low-frequency vibrations in the far-IR region.

Numerous recent experimental evidences (e.g., compressibility measurements,[20] dielectric relaxation,[23] solvatochromic shifts,[33a−d] NMR,[10c] simulations,[12d] and solvation dynamics[3−5]) indicate that even in a large water pool ($w_0 > 10$), the properties of the confined water differ from those of bulk water. In view of this large body of evidence it is not correct to expect a bulk-water-like behavior even in a large water pool. Perhaps, it is more reasonable to expect that there is a large variation of the properties of water molecules from the almost-bulk-like water at the core to the highly immobilized water molecules hydrogen bonded to the AOT headgroups. The variation is expected to be most rapid over the first few water layers near AOT.

In a water pool hydrogen bonding of water molecules to AOT headgroups disrupts water−water hydrogen bonding. Berne et al.[37] showed that the high dielectric constant of water arises from mutual polarization of water molecules attached by

hydrogen bonds. Because of the interruption of water−water hydrogen bonds, the dielectric constant (polarity) at the AOT−water interface is lower than that in bulk water or that in the core of the water pool. The micropolarity of the water pool has been measured using many solvatochromic probes.[33a−d] These measurements indicate that the polarity of the water pool even at a very high w_0 (>40) is lower than that of water and is close to that of alcohol.[33a−c]

We now consider the location of the DCM molecules. At $w_0 = 0$, when there is no water pool, the emission properties of DCM in an AOT reverse micelle are very different from those in *n*-heptane.[4a] This suggests that, even at $w_0 = 0$, DCM molecules do not stay in a heptane-like environment between the alkyl chains of the AOT. On addition of water to the reverse micelle, when a water pool is formed, the emission maximum of DCM gradually shifts from 550 nm at $w_0 = 0$ to 615 nm at $w_0 = 39.5$. The red shift in the emission maximum of DCM on addition of water indicates that DCM molecules are exposed to the water molecules of the water pool. Since DCM is not soluble in water but is soluble in an alcohol, we presume that DCM does not reside in the core of the water pool and stays in the alcohol-like region near the AOT interface.

We now examine the possibility of self-diffusion of the probe DCM. On electronic excitation DCM becomes more polar and presumably more soluble in the core of the water pool. As a result after excitation it may migrate from the AOT interface toward a more polar region of the water pool. Translational diffusion coefficients (D) of several organic probes in many organized assemblies have been obtained from fluorescence anisotropy decay.[34,35] In the organized assemblies D of several organic probes is found to be around 5×10^{-10} m^2 s^{-1}, which is close to those in bulk water.[36] Thus, according to the relation $\langle l^2 \rangle = 2Dt$, the probe DCM molecule travels 1 nm/ns inside the microemulsion.

We will now discuss the role of self-diffusion of the probe (DCM) in the time-dependent spectral width as shown in Figures 5 and 9 and Table 2. At $t = 0$, DCM molecules near AOT experience a large variation in the solvent environment and exhibit different emission maxima. (Note, there are about six water layers of thickness ~0.2 nm over the length, 1.25 nm, of the DCM molecule). All such DCM molecules are excited simultaneously. Due to the superposition of the emission spectra of DCM in different environments at short times, the spectral width is very large (Figure 9). Following electronic excitation DCM moves away from the AOT interface to the water pool. Thus, at long time, the emission spectrum originates from the DCM molecules at a relatively large distance from AOT. This corresponds to a more uniform environment and, hence, leads to a smaller spectral width. Thus, the decay of Γ with time may be ascribed to self-diffusion of the probe inside the water pool. It is likely that in the solvation dynamics in the water pool the rate-determining step is the diffusion of the probe from the AOT interface, where the bound water molecules are immobilized to a region quite distant from the AOT molecules where water molecules are quite free and exhibit ultrafast dynamics. Thus, the solvation dynamics in the water pool is controlled by the diffusion of the probe and is similar to the decay of Γ. It is readily seen from Tables 1 and 2 that the decay characteristics of $\Gamma(t)$ and $C(t)$ are remarkably similar. In summary, the slow components (100−1000 ps) in the decay characteristics of $\Gamma(t)$ and $C(t)$ in a water pool arise from self-diffusion of the probe.

However, one should note that self-diffusion of the probe is not the only source of the slow (100−1000 ps) components of the solvation dynamics for the following reasons. First, such slow components are also detected in dielectric relaxation and NMR studies, which are free from the complications due to translational diffusion of the fluorescent probe. Second, the secondary aggregate of Na-cholate in the bulk, which does not show time-dependent Γ, also exhibits slow solvation dynamics with $\langle \tau_s \rangle = 830$ ps. The lack of time dependence of Γ indicates self-diffusion of the probe is unimportant in this case. Thus, it seems that though probe diffusion seems to cause slow solvation dynamics and time-dependent decay of the spectral width in the case of microemulsions, this mechanism is not universally applicable and there are other sources of the slow component.

In systems (e.g., Na-cholate in bulk water) where self-diffusion is unimportant, the slow components of the solvation dynamics may arise from the dynamic exchange between "bound" and "free" water molecules.[11] As discussed by Nandi and Bagchi,[11] the magnitude of the slow component of relaxation depends on the free energy difference ($\Delta G°$) between bound and free water molecules. In the limit of very large $\Delta G°$, the slow component of relaxation (τ_{slow}) is given by $\tau_{slow} \approx k_{bf}^{-1}$, where k_{bf} is the rate constant for bound-to-free interconversion. k_{bf} is given by

$$k_{bf} = (k_B T/h) \exp[-(|\Delta G^*| + |\Delta G°|)/RT]$$

From this equation, the 830 ps component in the case of a bile salt aggregate in bulk water corresponds to $\Delta G° = -4.2$ kcal mol^{-1}.

More recently, there have been several computer simulations on the micelles,[12a,b] liquid−liquid interfaces,[12c] and microemulsions.[12d,e] These simulations predict a slower dynamics compared to that in bulk water. The simulations on a microemulsion carried out by Senapathy and Chandra[12d] indicate a retardation of the solvation dynamics by less than an order of a magnitude compared to that in bulk water and the dielectric constant of the water pool is smaller than that in bulk water by a factor 2. This is qualitatively consistent with the present work. However, it should be pointed out that none of the simulations considered probe diffusion. According to recent simulations,[38a,b] the water molecules in lipid vesicles and other surfactant assemblies form hydrogen bond bridges between surfactant molecules. Movement of these water molecules may involve "chain melting", and this may also give rise to the slow component of the solvation dynamics. The role of chain melting in the ultraslow component of the solvation dynamics in a biological system has not been considered so far.

We will now consider the effect of Na-sal and Na-cholate on the solvation dynamics in the water pool. The faster solvation dynamics in the case of Na-sal may be explained as follows. Because of diffusion, the DCM molecule undergoes excursion over a region within the water pool and monitors the dynamics of both the very slow tightly bound peripheral water molecules near the AOT headgroups and the relatively more mobile water molecules at a large distance from AOT. In a bigger pool, the contribution of the fast water molecules is larger and, hence, solvation is faster. Thus, the 2-fold acceleration on addition of 1 mM Na-sal may be ascribed to the larger size of the water pool.[3,4] On addition of 100 mM Na-cholate, the radius of the water pool increases about 2 times and, thus, one may expect faster dynamics. But in this case, in each water pool there are 550 Na-cholate molecules which may form aggregates. Though aggregates of bile salts are studied in bulk water,[29a] very little is known about their aggregation behavior within the confined water pool of AOT microemulsions (i.e., "a micelle within a micelle"). The presence of such aggregates of Na-cholate makes the water pool very crowded. The crowding may cause

retardation in diffusion of the probe inside the water pool of microemulsions in the presence of Na-cholate and may be responsible for the slower solvation dynamics compared to that in the absence of Na-cholate.

Finally, we will discuss why DCM does not show time dependence of Γ in the secondary aggregate of Na-cholate in bulk water. According to a SANS study, the secondary aggregate of Na-cholate in bulk water (at a concentration above 50 mM) resembles an elongated rod with a central hydrophilic core filled with water and ions.[29c] Since DCM is insoluble in bulk water, in this case the DCM molecules are constrained to remain within the narrow hydrophilic core. The hydrophilic core is of length 3.6 nm and diameter 1.6 nm.[29c] This is barely larger than the DCM molecule (length 1.25 nm). The observed solvation time of 830 ps in this case would correspond to translation over a distance of 0.83 nm, and even if the excited probe molecule undergoes translation over this distance, it would be inside the hydrophilic core and would experience the same environment. This could be the reason for the lack of time dependence of the spectral width in this case.

5. Conclusion

The solvation dynamics in the water pool of an AOT microemulsion is markedly influenced by the addition of Na-sal and Na-cholate. In a microemulsion the Γ of the time-dependent emission spectra decreases quite dramatically with an increase in time, while no such time-dependent spectral width is detected in bulk water in the case of a bile salt (Na-cholate) aggregate. The decay of Γ and solvation dynamics in the case of a microemulsion has been ascribed to the self-diffusion of the fluorescent probe (DCM) from the relatively nonpolar AOT interface toward the core of the water pool. Addition of 1 mM Na-sal to the AOT microemulsion causes an increase in the size of the water pool, and the solvation dynamics becomes faster because of the contribution of the faster water molecules at a distance from AOT. In bulk water, at a concentration of 100 mM, Na-cholate forms secondary aggregates and exhibits a solvation time of 830 ps. However, the solvation dynamics is 4 times slower in the water pool of an AOT microemulsion in the presence of 100 mM Na-cholate, with a solvation time of 3050 ps. This is attributed to the very crowded environment within the water pool because of the presence of aggregates of Na-cholate. This result has biological implications as in a biological cell various processes occur in a confined and crowded environment. In the case of Na-cholate aggregates in bulk water, the lack of a time-dependent spectral width indicates self-diffusion of the probe is unimportant and the slow solvation arises entirely from the dynamic exchange between bound and free water.[11]

Acknowledgment. Thanks are due to the Council of Scientific and Industrial Research (CSIR) and Department of Science and Technology (DST), Government of India, for generous research grants. P.D. and A.H. thank the CSIR for awarding fellowships, and P.S. thanks the DST for awarding a fellowship. K.B. thanks Professor B. Bagchi for many stimulating discussions.

References and Notes

(1) (a) Jordanides, X. J.; Lang, M. J.; Song, X.; Fleming, G. R. *J. Phys. Chem. B* **1999**, *103*, 7995. (b) Pal, S. K.; Peon, J.; Zewail, A. H. *Proc. Natl. Acad. Sci. U.S.A.* **2002**, *99*, 1763. (c) Mandal, D.; Sen, S.; Sukul, D.; Bhattacharyya, K.; Mandal, A. K.; Banerjee, R.; Roy, S. *J. Phys. Chem. B* **2002**, *106*, 10741. (d) Pal, S. K.; Mandal, D.; Sukul, D.; Sen, S.; Bhattacharyya, K. *J. Phys. Chem. B* **2001**, *105*, 1438.

(2) (a) Brauns, E. B.; Madaras, M. L.; Coleman, R. S.; Murphy, C. J.; Berg, M. A. *Phys. Rev. Lett.* **2002**, *88*, 158101−1. (b) Brauns, E. B.; Madaras, M. L.; Coleman, R. S.; Murphy, C. J.; Berg, M. A. *J. Am. Chem. Soc.* **1999**, *121*, 11644.

(3) (a) Willard, D. M.; Riter, R. E.; Levinger, N. E. *J. Am. Chem. Soc.* **1998**, *120*, 4151. (b) Riter, R. E.; Willard, D. M.; Levinger; N. E. *J. Phys. Chem. B* **1998**, *102*, 2705.

(4) (a) Pal, S. K.; Mandal, D.; Sukul, D.; Bhattacharyya, K. *Chem. Phys. Lett.* **1999**, *312*, 178. (b) Sarkar, N.; Das, K.; Datta, A.; Das, S.; Bhattacharyya, K. *J. Phys. Chem.* **1996**, *100*, 10523. (c) Lundgren, J. S.; Heitz, M. P.; Bright, F. V. *Anal. Chem.* **1995**, *67*, 3775. (d) Bhattacharyya, K.; Hara, K.; Kometani, N.; Yozu, Y.; Kajimoto, O. *Chem. Phys. Lett.* **2002**, *361*, 136. (e) Sen, S.; Dutta, P.; Sukul, D.; Bhattacharyya, K. *J. Phys. Chem. A* **2002**, *106*, 6017.

(5) (a) Riter, R. E.; Undiks, E. P.; Kimmel, J. R.; Pant, D. D.; Levinger, N. E. *J. Phys. Chem. B* **1998**, *102*, 7931. (b) Shirota, H.; Horie, K. *J. Phys. Chem. B* **1999**, *103*, 1437.

(6) (a) Sykora, J.; Kapusta, P.; Fidler, V.; Hof, M. *Langmuir* **2002**, *18*, 571. (b) Pal, S. K.; Sukul, D.; Mandal, D.; Bhattacharyya, K. *J. Phys. Chem. B* **2000**, *104*, 4529.

(7) (a) Sen, S.; Sukul, D.; Dutta, P.; Bhattacharyya, K. *J. Phys. Chem. B* **2002**, *106*, 3763. (b) Frauchiger, L.; Shirota, H.; Uhrich, K. E.; Castner, E. W., Jr. *J. Phys. Chem. B* **2002**, *106*, 7463.

(8) Loughnane, B. J.; Farrer, R. A.; Scodinu, A.; Reilly, T.; Fourkas, J. T. *J. Phys. Chem. B* **2000**, *104*, 5421.

(9) (a) Jordan, J. D.; Dunbar, R. A.; Bright, F. V. *Anal. Chem.* **1995**, *67*, 2436. (b) Pal, S. K.; Sukul, D.; Mandal, D.; Sen, S.; Bhattacharyya, K. *J. Phys. Chem. B* **2000**, *104*, 2613. (c) Baumann, R.; Ferrante, C.; Deeg, F. W.; Bräuchle, C. *J. Chem. Phys.* **2001**, *114*, 5781.

(10) (a) Otting, G.; Liepinsh, E.; Wuthrich, K. *Science* **1991**, *254*, 974. (b) Denisov, V. P.; Jonsson, B.-H.; Halle, B. *Nat. Struct. Biol.* **1999**, *6*, 253. (c) Carlstrom, G.; Halle, B. *Langmuir* **1988**, *4*, 1346.

(11) Nandi, N.; Bagchi, B. *J. Phys. Chem. B* **1997**, *101*, 10954.

(12) (a) Balasubramanian, S.; Pal, S.; Bagchi, B. *Phys. Rev. Lett.* **2002**, *89*, 115505−1. (b) Balasubramanian, S.; Bagchi, B. *J. Phys. Chem. B* **2002**, *106*, 3668. (c) Michael, D.; Benjamin, I. *J. Chem. Phys.* **2001**, *114*, 2817. (d) Senapathy, S.; Chandra, A. *J. Chem. Phys.* **1999**, *111*, 1223. (e) Faeder, J.; Albert, M. V.; Ladanyi, B. M. *Langmuir* **2003**, *19*, 2514.

(13) (a) Pal, S. K.; Peon, J.; Bagchi, B.; Zewail, A. H. *J. Phys. Chem. B* **2002**, *106*, 12376. (b) Bhattacharyya, K. *Acc. Chem. Res.* **2003**, *36*, 95. (c) Bhattacharyya, K.; Bagchi, B. *J. Phys. Chem. A* **2000**, *104*, 10603. (d) Nandi, N.; Bhattacharyya, K.; Bagchi, B. *Chem. Rev.* **2000**, *100*, 2013. (e) Levinger, N. E. *Curr. Opinion Colloid Interface Sci.* **2000**, *5*, 118.

(14) Borkovec, M.; Eicke, H.-F. *Chem. Phys. Lett.* **1989**, *157*, 457.

(15) Zulauf, M.; Eicke, H.-F. *J. Phys. Chem.* **1979**, *83*, 480.

(16) Ricka, J.; Borkovec, M.; Hofmeier, U. *J. Chem. Phys.* **1991**, *94*, 8503.

(17) Maitra, A. *J. Phys. Chem.* **1984**, *88*, 5122.

(18) Moulik, S. P.; De, G. C.; Bhowmik, B. B.; Panda, A. K. *J. Phys. Chem. B* **1999**, *103*, 7122.

(19) Nazario, L. M. M.; Hatton, T. A.; Crespo, J. P. S. G. *Langmuir* **1996**, *12*, 6326.

(20) Amararene, A.; Gindre, M.; Le Huerou, J.-Y.; Nicot, C.; Urbach, W.; Waks, M. *J. Phys. Chem. B* **1997**, *101*, 10751.

(21) Venables, D. S.; Huang, K.; Schmuttenmauer, C. A. *J. Phys. Chem. B* **2001**, *105*, 9132.

(22) (a) Peyrelasse, J.; Boned, C. *J. Phys. Chem.* **1985**, *89*, 370. (b) Peyrelasse, J.; Boned, C. *Phys. Rev. A* **1990**, *41*, 938.

(23) D'Angelo, M.; Fioretto, D.; Onori, G.; Palmieri, L.; Santucci, A. *Phys. Rev. E* **1996**, *54*, 993.

(24) (a) Boyd, J. E.; Briskman, A.; Sayes, C. M.; Mittleman, D. M. Colvin, V. L. *J. Phys. Chem. B* **2002**, *106*, 6346. (b) Mittleman, D. M.; Nuss, M. C.; Colvin, V. L. *Chem. Phys. Lett.* **1997**, *275*, 332.

(25) (a) Jarzeba, W.; Walker, G. C.; Johnson, A. E.; Kahlow, M. A.; Barbara, P. F. *J. Phys. Chem.* **1988**, *92*, 7039. (b) Jimenez, R.; Fleming, G. R.; Kumar, P. V.; Maroncelli, M. *Nature* **1994**, *369*, 471. (c) Nandi, N.; Roy, S.; Bagchi, B. *J. Chem. Phys.* **1995**, *102*, 1390.

(26) (a) Mayer, M.; Mialocq, J.-C. *Opt. Commun.* **1987**, *64*, 264. (b) Hsing-Kang, Z.; Ren-Lan, M.; Er-pin, N.; Chu, G. *J. Photochem.* **1985**, *29*, 397.

(27) (a) Jonkman, M.; van der Meulen, P.; Zhang, H.; Glasbeek, M. *Chem. Phys. Lett.* **1996**, *256*, 21. (b) Easter, D. C.; Baronavski, A. P. *Chem. Phys. Lett.* **1993**, *201*, 153. (c) Gustavsson, T.; Baldacchino, G.; Mialocq, J.-C.; Pommeret, S. *Chem. Phys. Lett.* **1995**, *236*, 587. (d) van der Meulen, P.; Zhang, H.; Jonkman, A. M.; Glasbeek, M. *J. Phys. Chem.* **1996**, *100*, 5367.

(28) Sen, S.; Dutta, P.; Mukherjee, S.; Bhattacharyya, K. *J. Phys. Chem. B* **2002**, *106*, 7745.

(29) (a) Small, D. M. *The Bile Acid*; Plenum: New York, 1971; Vol. 1, p 302. (b) Ju, C.; Bohne, C. *J. Phys. Chem.* **1996**, *100*, 3847. (c)

Santhanlakshmi, J.; Shantha Lakshmi, G.; Aswal, V. K.; Goyal. P. S. *Proc. Indian Acad. Sci. (Chem. Sci.)* **2001**, *113*, 55.

(30) (a) Horng, M.-L.; Gardecki, J. A.; Maroncelli, M. *J. Phys. Chem. A* **1997**, *101*, 1030. (b) Maroncelli, M.; Fleming, G. R. *J. Chem. Phys*. **1987**, *86*, 6221. (c) Maroncelli, M. *J. Mol. Liq.* **1993**, *57*, 1.

(31) Bart, E.; Melstein, A.; Huppert, D. *J. Phys. Chem*. **1995**, *99*, 9253.

(32) (a) Mandal, D.; Datta, A.; Pal, S. K.; Bhattacharyya, K. *J. Phys. Chem. B* **1998**, *102*, 9070. (b) Pant, D.; Levinger, N. E. *Langmuir* **2000**, *16*, 10123.

(33) (a) Datta, A.; Mandal, D.; Pal, S. K.; Bhattacharyya, K. *J. Phys. Chem. B* **1997**, *101*, 10221. (b) Guha Ray, J.; Sengupta, P. K. *Chem. Phys. Lett.* **1994**, *230*, 75. (c) Mandal. D.; Pal, S. K.; Datta, A.; Bhattacharyya, K. *Anal. Sci.* **1998**, *14*, 199. (d) Cho, C. H.; Chung, M.; Lee, J.; Nguyen, T.; Singh, S.; Vedamuthu, M.; Yao, S.; Zhu, S.-B.; Robinson, G. W. *J. Phys. Chem.* **1995**, *99*, 7806.

(34) (a) Quitevis, E. L.; Marcus, A. H.; Fayer, M. D. *J. Phys. Chem.* **1993**, *97*, 5762. (b) Maiti, N. C.; Krishna, M. M. G.; Britto, P. J.; Periasamy, N. J. *J. Phys. Chem. B* **1997**, *101*, 11051. (c)Wittouck, N. W.; Negri, R. M.; De Schryver, F. C. *J. Am. Chem. Soc.* **1994**, *116*, 10601.

(35) Sen, S.; Sukul, D.; Dutta, P.; Bhattacharyya, K. *J. Phys. Chem. A* **2001**, *105*, 7495.

(36) For example, D of *p*-aminobenzoic acid is 8×10^{-10} m^2 s^{-1}: *Handbook of Chemistry and Physics*; CRC Press: Boca Raton, FL, 1990; pp 6−151.

(37) Rick, S. W.; Stuart, S. J.; Berne, B. J. *J. Chem. Phys*. **1994**, *101*, 6141.

(38) (a) Pasenkiewicz-Gierula, M.; Takaoka, V.; Miyagawa, H.; Kitamura, K.; Kusumi, A. *J. Phys. Chem. A* **1997**, *101*, 3677. (b) Bandyopadhyay, S.; Tarek, M.; Lynch, M. L.; Klein, M. L. *Langmuir* **2000**, *16*, 942.